Rev. Téc. Ing. Univ. Zulia. Vol. 32, Nº 3, 210 - 221, 2009

New U-Pb zircon ages of El Baúl Massif, Cojedes State, Venezuela

Patxi Viscarret[1]*, James Wright[2] and Franco Urbani[3]

[1]Grupo de Investigación de Ciencias de la Tierra-TERRA, Escuela de Ingeniería Geológica, Universidad de Los Andes. Mérida, Venezuela. patxi@ula.ve
[2]Department of Geology, The University of Georgia. Athens, Georgia, 30602-2501, USA.
[3]Escuela de Geología, Minas y Geofísica, Universidad Central de Venezuela, Caracas and Fundación Venezolana de Investigaciones Sismológicas (FUNVISIS). Prolongación calle Mara, El Llanito, Caracas, Venezuela

Abstract

El Baúl massif (Cojedes State, Venezuela) has been studied since 1858, especially as an important target for oil companies since it is a structural high that has played an important role in the evolution of the oil bearing Barinas-Apure and Eastern Venezuela sedimentary basins. In addition, igneous and metamorphic rocks have received attention to understand the evolution and relationships of the granitic bodies and their enveloping rock. Prior to this study the Mogote Granite was considered Permian, based on two ages of 287 ± 10 Ma Rb/Sr and 270 ± 10 Ma K/Ar, while the Guacamayas volcanics, were considered Early Jurassic, also for two K/Ar ages (192 ± 3.8 Ma and 195 ± 3.9 Ma). Due to the currently known unreliability of these ages obtained decades ago, new work was done where five new U-Pb zircon ages, in the granitic and volcanic rocks were obtained with the SHRIMP-RG method. The new ages are: El Corcovado Rhyolite, 286.4 ± 2.8 Ma and La Segoviera Rhyolite, 283.3 ± 2.5 Ma (Early Permian), both of the Guacamayas Super Suite. For El Baúl Granitic Suite were obtained ages for: Piñero Granite (289.0 ± 2.9 Ma) and Mata Oscura Granite (294.1 ± 3.1 Ma), both Early Permian, whereas the Mogote Granite (493.8 ± 5.2 Ma) is Late Cambrian. These new ages show that the El Baúl massif forms part of an igneous and metamorphic Paleozoic belt, with features more similar to the known geology of the Merida Andes and the Coastal mountains than to the Guyana Shield as previously postulated. Besides it does not appear to behave as an "Arch "spreading from the Guyana Shield up to the Paraguaná peninsula, as previously thought.

Key words: El Baúl massif, geochronology, SHRIMP-RG, Venezuela, zircon.

Nuevas edades U-Pb en circones para el macizo El Baúl, estado Cojedes, Venezuela

Resumen

El macizo de El Baúl (estado Cojedes, Venezuela) ha sido muy estudiado desde 1858 hasta el presente, especialmente como un objetivo importante de investigaciones por parte de empresas petroleras, ya que como un elemento de alto estructural, ha jugado un papel relevante en la evolución de las cuencas sedimentarias Barinas-Apure y del Oriente de Venezuela. Adicionalmente, las rocas ígneas y metamórficas han recibido atención para entender la evolución y relaciones de campo entre los cuerpos graníticos y su roca caja. Previamente el Granito de Mogote era considerado Pérmico, basado en una edad de 287 ± 10 Ma Rb/Sr y una de 270 ± 10 Ma K/Ar, y las rocas volcánicas de Guacamayas eran consideradas como Jurásico Temprano igualmente por dos edades K/Ar (192 ± 3,8 Ma y 195 ± 3,9 Ma). Debido a la poca confiabilidad atribuida actualmente a estas edades obtenidas décadas atrás en las rocas graníticas y volcánicas, se realizó un trabajo donde se obtuvieron cinco nuevas edades U-Pb en circón con el método SHRIMP-RG.

Las nuevas edades son: Riolita de El Corcovado: 286,4 ± 2,8 Ma y Riolita de La Segoviera: 283,3 ± 2.5 Ma, es decir Pérmico Temprano, ambas de la Super-Asociación Guacamayas. Para la Asociación Granítica El Baúl se obtuvieron edades para el Granito de Piñero (289,0 ± 2,9 Ma) y el Granito de Mata Oscura (294,1 ± 3,1 Ma), resultando ambas del Pérmico Temprano, mientras que sorpresivamente, el Granito de Mogote (493,8 ± 5,2 Ma), resultó del Cámbrico Tardío. Estas nuevas edades permiten interpretar que el macizo de El Baúl forma parte de un cinturón Paleozoico de rocas ígneas y metamórficas, con características mas afines a la geología conocida de la Cordillera de los Andes de Mérida y la Costa, que al escudo de Guayana. Además no parece comportarse como un "Arco" que va desde el cratón de Guayana hasta la península de Paraguaná, como se interpretó previamente.

Palabras clave: Circón, geocronología, macizo El Baúl, SHRIMP-RG, Venezuela.

Introduction

The Baúl massif is located in the southwestern part of the Cojedes state, close to the village of El Baúl, 60 km south of the El Pao town (Figure 1), in north-central Venezuela and north of the Guyana Shield. The area is isolated and mountainous with steep topography, that follows a northwest-southeast trend and cover an area of about 720 km^2. It emerges as a geomorphologic-structural high between the Barinas-Apure, and the Eastern Venezuelan sedimentary basins. Martín [1] differentiated several units and subunits of three rocks types, namely: granitic, volcanic and metasedimentary.

This massif is associated with a distensional tectonic deformational front, to the south and another compressional to the north [4]. Precambrian and Palaeozoic rocks form the basement, from the Perija Range and at least the Colombian Llanos to the west, until Anzoátegui state in eastern Venezuela (Figure 2). Paleozoic sedimentation took place between two major orogenies called Taconic (≈ 600-430 Ma) and Appalachian (≈ 360-270 Ma) equivalent to the European Caledonian and Hercinian, respectively, such events changed the nature and distribution of pre-existing rocks [4].

The goal of this work has been to obtain new radiometric ages, for the El Baúl massif igneous rocks, applying the new technology SHRIMP-RG in U-Pb geochronology in zircon crystals. The new data can be used to improve new petrogenetic models.

Geology of the massif area

The nomenclature of geological units of the massif has been updated following the rules of lithodemic units [5], as follows [6]: 1) Metasedimentary rocks: Barbasco Metasedimentary Suite (Cañaote Quartzite, Cerrajón Metapelite), Mireles

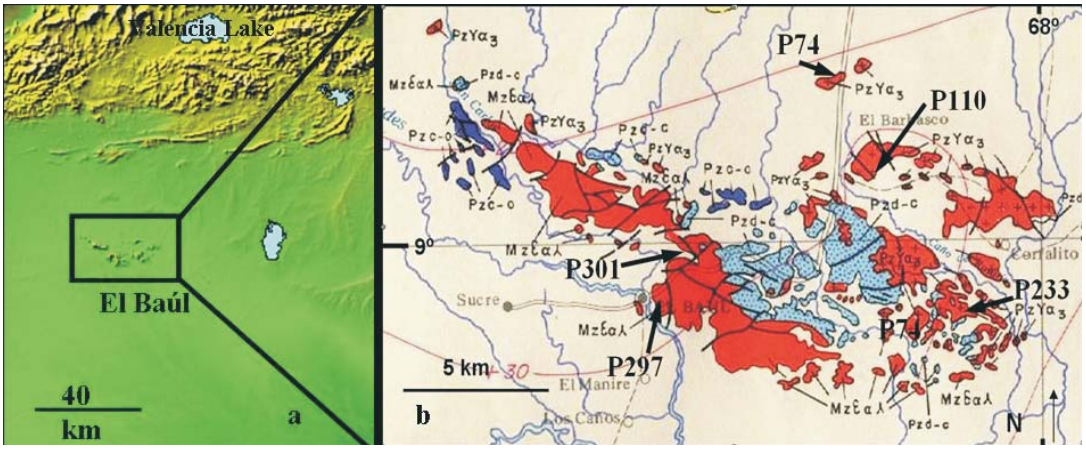

Figure 1. (a) Location [2] and geological map [3] of El Baúl massif, Cojedes state, Venezuela. Arrows indicate sample locations. Pzc-o and Pzd-c: Paleozoic, Mireles Slate and metasedimentary respectively; PzYα3: Paleozoic, granitoids and Mzελ, Mesozoic, Volcanic Guacamayas Group.

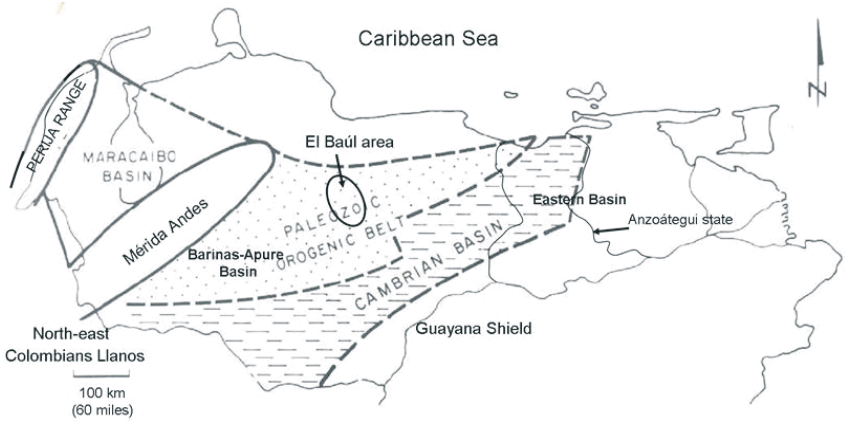

Figure 2. El Baúl massif located to the north of the Guyana Shield and between the Eastern and Apure-Barinas sedimentary basins [4].

Phyllite (with Cambrian-Ordovician trilobites); 2) Volcanic rocks: Guacamayas Super-Suite: Teresén Rhyolitic Suite (Corcovado Rhyolite, Tirado Rhyolite, La Bandola Rhyolite), El Peñón Latitic Suite (El Oso Quartz Latite, Segoviera Rhyolite); and 3) El Baúl Granitic Suite (Piñero Granite, Mata Oscura Granite and Mogote Granite).

Martin [1] divided the metasedimentary rocks in three sections: a lower section (Mireles Phyllite) essentially phyllitic and fossiliferous metalimolite; an intermediate (Cerrajón Metapelite) with interlayering of sterile quartzite, exposed in the central and north central parts of the massif; and a top sterile (Cañaote Quartzite), of medium to coarse grain quartzite, exposed in the southwestern parts. The contacts between them are transitional while the contact with the basal section of volcanic Guacamayas Super-Suite is an unconformity or by fault.

The Guacamayas Volcanic rocks have been grouped from old to young in: a) Teresén Rhyolitic Suite composed by flows of rhyolitic lavas interlayered with ash tuffs, agglomerate and sandstone, whose stratigraphic relations allow to separate three volcanic episodes with its pyroclastics equivalent, that from bottom up are: Corcovado Rhyolite, Tirado Rhyolite and La Bandola Rhyolite; b) El Peñón Latitic Suite is composed by a sequence of porphyritic latitic lavas and flows of glassy tuffs that culminate in a thick accumulation of tuffs and agglomerates; it is divided in two subunits (El Oso Quartz Latite, Segoviera Rhyolite) with transitional contact between them. These groups have a minimal thickness of 450 m. Its lower contact is faulted with the Cañaote Quartzite of the Barbasco Metasedimentary Suite while its upper one is unknown, since there are no vestiges of overlying sediments.

From El Baúl granitoid units, Mogote Granite has been considered the external mass of the batholith [1]. It is greyish pink with porphidic to pegmatitic and rapakivi (K-feldspar phenocrystal up to 12 cm) textures. The Mata Oscura Granite occurs in the middle of the batholith, with coarse equigranular grains of flecked salmon and greenish grey colour, and represents the dominant unit of the region. The Piñero Granite occupies the smaller area of the granitic bodies, and has been considered to be the youngest. It is fine to medium grained and of salmon pink colour and darkly specked.

Associated with the granitoids, there are late intrusions of syenite, aplite, diorite and diabase. The syenite represents a marginal event of the batholith, of which it constitutes scarcely a 5% of the area; it grades from medium grain size to pegmatitic. Aplite dikes are persistent, white and present thicknesses of up to 10 m. The diorite and diabase appear as dikes or apophyse of centimetric to decimetric thickness and moderate extension and intrude the Mata Oscura and Piñero granites. They are dark coloured, dense and with porphyritic texture. The granitic rocks are in fault contact with the red metapelitic rocks of El Barbasco Metasedimentary Suite. The granitoids and the metasedimentary rocks are

intruded by rhyolite dikes of the Guacamayas Super-Suite, with no genetic relations with the granite magmatic events.

Martín [1] interpreted that El Baúl granitoids were slowly emplaced in a non orogenic time (post-orogenic) and shallow depth, which allowed segregation in the magmatic chamber and were emplaced in the folded and faulted metasedimentary rocks of El Barbasco metasediments. The Guacamayas volcanic rocks are post-orogenic and fissural, partially subaquatic.

Previous Geochronology

For the Mogote Granite, two radiometric ages were available: 270 ± 10 Ma K/Ar and 287 ± 10 Ma Rb/Sr [7] that is, Pennsylvanian to Early Permian. Macdonald [8] determined ages of 192 ± 3.8 Ma and 195 ± 3.9 My K/Ar for rhyolite samples (Segoviera Rhyolite) of the Guacamayas volcanics, which locates the age of this suite in the Early Jurassic. These ages suggested that: 1) the massif had an Ordovician metasedimentary basal unit, dated with trilobites; 2) At the end of the Appalachian orogeny (that began 360 Ma and finished approximately 270 Ma ago), the granitoids were emplaced in the metasediments as a post orogenic event. 3) In Jurassic time, volcanic rocks intruded the earlier granites and deposited also as thick lava flows [1].

So this previous age control of El Baúl rocks has hampered the development of a consistent tectonic model for this area. The previous K/Ar methods used three decades ago are not considered reliable since isotopic content is very susceptible to changes by hydrothermal events which are evident in the zone, and are also susceptible to be changed due to tectonism such as shearing and cataclastic events which we have documented in the petrographic analysis. Therefore, it was deemed necessary to obtain new geochronologic data using the U-Pb method in zircons.

Analytical Methods

In this study, we report ages of grains of zircon. U-Pb geochronology was performed using the U.S. Geological Survey/Stanford University Sensitive High Resolution Ion Microprobe-Reverse Geometry (SHRIMP-RG) facility. Seven samples from 10-15 kg were collected in the following units (see samples localities in Figure 1):

Volcanic rocks: In Corcovado Rhyolite (sample P297) and Segoviera Rhyolite (sample P301) extraction and dating of zircons were successful. In La Bandola Rhyolite (sample P298) and El Oso Quartz Latite (sample P299) no crystals of zircon could be extracted.

Granitic rocks: In Piñero Granite (sample P233), Mata Oscura Granite (P110) and Mogote Granite (P74) extraction of zircon and age determination were successful. These granitic rocks are compact, equigranular and contain pink to salmon-coloured K-feldspar. The grain size varies from fine in Piñero Granite, to medium and coarse in Mata Oscura Granite, and even coarser (up to 10 cm) in Mogote Granite. The latter unit also displays a rapakivi like texture.

The samples were processed in the Laboratory of Isotope Geology at The University of Georgia (Athens, USA). Crystals of zircon were extracted using standard mineral-separation techniques and then sorted according to their magnetic susceptibility using a Frantz isodynamic separator. Individual grains were hand picked and selected under a binocular microscope to avoid inclusions and other imperfections. Latter were mounted in a 2.5 cm epoxy disc including grains of standard zircon CZ3 [9], them were ground to half-thickness to expose internal zones and polished using 6 μm and 1 μm diamond suspension and coated (~10 nm) of high purity Au [10]. Scanning electron microscope (SEM) images were obtained to characterize the internal structures of the zircon grains, and these images were used to position the ion beam.

The SHRIMP-RG analysis followed the methods of Williams [11]. We used a primary oxygen beam at a current of about 4 nA, which excavates pits of about 25 to 35 μm in diameter and about 1 μm in depth. The resulting material enters the mass spectrometer [18] and isotopic U-Pb compositional data were obtained. The primary beam was rastered across the analytical spot for 90-120s before analysis to reduce the proportion of common Pb. The secondary ion mass spectrum is dominated by ions consisting of one or two metal atoms in combination with one, two or three oxygen atoms. The magnet cy-

cled through the mass stations six times per analysis. The raw data were plotted using the software Isoplot 3 [12].

The ratios and absolute abundances of U, Th and Pb isotopes were determined relative to the CZ3 zircon standard ($^{206}Pb/^{238}U$ = 0.09143 (564 Ma), 550 ppm ^{238}U), using the operating and data-processing procedures described by [13, 14]. Zircon CZ3 has been selected as a U-Pb geochronology standard for SHRIMP analyses because of its homogeneity in terms of U and Pb [15]. Different areas in the grains zircon were interspersed and analyzed in conjunction with the CZ3, to verify the accuracy of the U-Pb calibration. Data reduction and error follow methods outlined in [16] and [17]. Zircon spot ages are reported at the 1σ level, but interpreted ages of crystallization of the rocks are reported as the weighted mean age at the 2σ level.

The beam took samples in different zones of the zircons grains [18] and isotopic U-Pb compositional data were obtained by de SHRIMP-RG.

New Geochronology

On the basis of SEM images, sample P297 (Corcovado Rhyolite) (Figure 3) shows a homogeneous population of short prismatic crystals of zircon, between 60 and 110 μm in length, anhedral to subhedral with pyramidal faces. Incipient overgrowth zoning appears near the edge of the grains. Twelve crystals of zircon were analyzed from this sample (Table 1) and the isotopic information was reported on a Concordia graph (Figure 4). Most of the data points are concordant and are consistent with a $^{206}Pb/^{238}U$ age of 286.4 ± 2.8 Ma.

In sample P301 (Segoviera Rhyolite; Figure 5), the crystals of zircon are morphologically similar to the pevious sample, and range between 70 and 110 μm in length.

Eight crystals of zircon were analyzed (Table 2) and the isotopic data was plotted in a Concordia graph (Figure 4). The points are concordant and give a $^{206}Pb/^{238}U$ age of 283.3 ± 2.5 Ma. So de two volcanic units are of Early Permian age.

The granite samples yielded homogeneous populations of prismatic euhedral grains with well developed oscillatory zoning, in some cases with an irregular core without clear definition of inherited zircon. In samples P233 (Piñero Granite, Figure 6) and P110 (Mata Oscura Granite, Figure 7), the grains range from 80 to 200 μm in length. Some zircon grains of Mata Oscura Granite have metamict zones.

Twelve crystals of zircon were analyzed from each sample (Tables 3 and 4) and the data were drawn on Concordia plots. Most of the data points are concordant, with a $^{206}Pb/^{238}U$ age of 289 ± 2.9 Ma for Piñero Granite (Table 3) and 294.1 ± 3.1 Ma for Mata Oscura Granite (Figure 8). Therefore these units are Early Permian.

Mogote granite sample (P74) yielded homogeneous populations of prismatic euhedral grains, whose size ranges from 200 to 300 μm in length with less regular oscillatory zoning

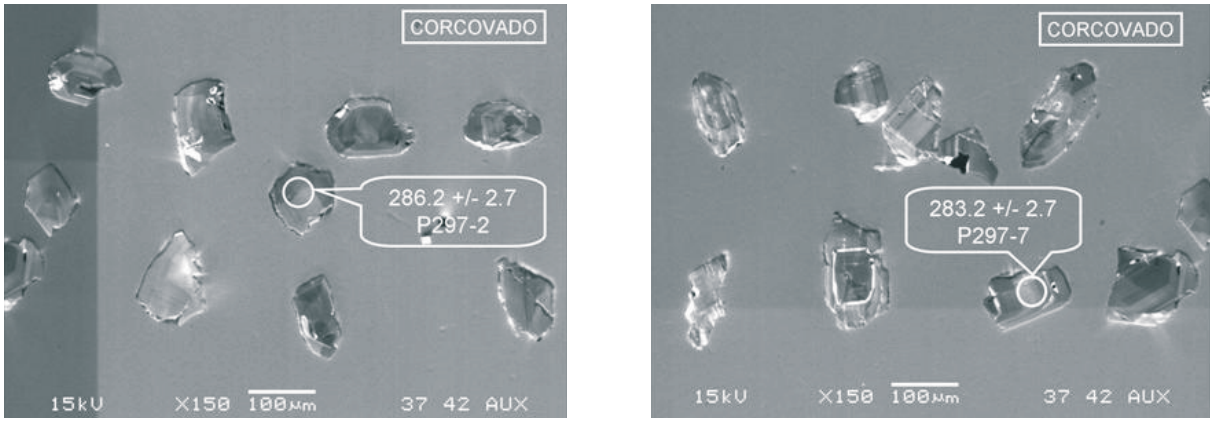

Figure 3. Selected zircon SEM images for Corcovado Rhyolite (P297) samples. The SHRIMP-RG determinations were made in the circle areas.

Table 1
Corcovado Rhyolite (P297) isotopic SHRIMP-RG zircon data

Spot	% $^{206}Pb_c$	ppm U	$^{232}Th/^{238}U$	$^{206}Pb/^{238}U$ Age		$^{238}U/^{206}Pb^*$	±%	$^{207}Pb^*/^{206}Pb^*$	±%	$^{207}Pb^*/^{235}U$	±%	$^{206}Pb^*/^{238}U$	±%
P297-1	-	633	0,60	284.1	±2.6	22.19	0.94	0.05061	2	0.3144	2.2	0.04506	0.94
P297-2	0,10	598	0,50	286.2	±2.7	22.02	0.95	0.05234	1.8	0.3276	2	0.0454	0.95
P297-3	0,06	817	0,60	284.2	±2.5	22.19	0.91	0.05191	1.7	0.3226	1.9	0.04507	0.91
P297-4	-	470	0,51	280.8	±2.7	22.46	0.98	0.05164	1.8	0.317	2.1	0.04452	0.98
P297-5	0,08	377	0,45	278.9	±2.8	22.62	1	0.0518	2.3	0.3156	2.5	0.04422	1
P297-6	0,02	542	0,57	282.3	±2.7	22.34	0.96	0.05211	1.9	0.3216	2.1	0.04476	0.96
P297-7	0,11	520	0,57	283.2	±2.7	22.27	0.97	0.052	2	0.3223	2.3	0.04491	0.97
P297-8	-	482	0,53	288.9	±2.8	21.82	10	0.0498	2.4	0.315	2.6	0.04584	10
P297-9	-	859	0,71	282.6	±2.5	22.31	0.9	0.05164	1.4	0.3191	1.6	0.04482	0.9
P297-10	0,10	404	0,47	281.7	±2.8	22.39	1	0.0527	2	0.3247	2.2	0.04467	1
P297-11	0,16	519	0,56	281.8	±2.7	22.38	0.98	0.052	2.1	0.3202	2.4	0.04468	0.98
P297-12	0,08	432	0,52	283.6	±2.8	22.24	1	0.05262	1.9	0.3263	2.1	0.04497	1

Pb_c and Pb* indicate the common and radiogenic portions of plumb, respectively. Common Pb corrected using measured ^{204}Pb; ppm U: Uranium part per million; Spot: Zircon sample dated.

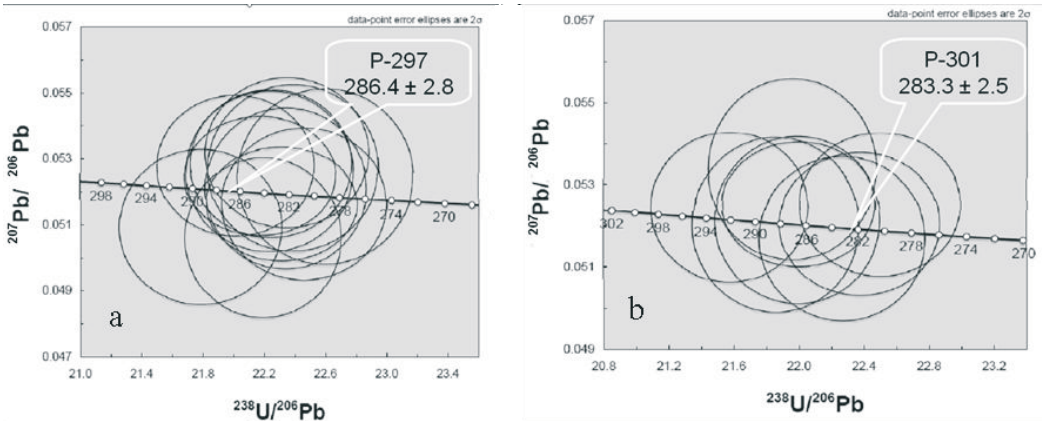

Figure 4. Concordia diagram for (a) Corcovado Rhyolite and (b) Segoviera Rhyolite.

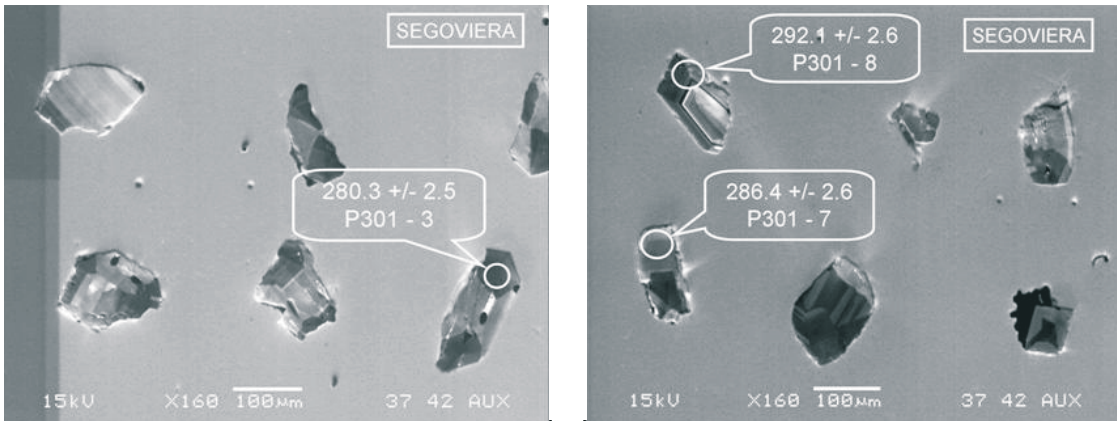

Figure 5. Selected zircon SEM images for Segoviera Rhyolite (P301).

Table 2
Segoviera Rhyolite (P301) isotopic SHRIMP-RG zircon data

Spot	% $^{206}Pb_c$	ppm U	$^{232}Th/^{238}U$	$^{206}Pb/^{238}U$ Age		$^{238}U/^{206}Pb^*$	±%	$^{207}Pb^*/^{206}Pb^*$	±%	$^{207}Pb^*/^{235}U$	±%	$^{206}Pb^*/^{238}U$	±%
P301-1	-	653	0,72	283.1	±2.6	22.28	0.94	0.0513	1.7	0.3175	1.9	0.04489	0.94
P301-2	0,17	550	0,52	287.1	±2.7	21.96	0.96	0.05339	1.7	0.3352	1.9	0.04554	0.96
P301-3	0,08	837	0,78	280.3	±2.5	22.5	0.9	0.05252	1.4	0.3219	1.6	0.04445	0.9
P301-4	-	563	0,63	288	±2.7	21.89	0.96	0.0508	2.1	0.3202	2.3	0.04568	0.96
P301-5	0,02	872	0,72	281.7	±2.5	22.39	0.9	0.05144	1.6	0.3168	1.8	0.04466	0.9
P301-6	0,06	1157	1,00	286.5	±2.4	22	0.87	0.0523	1.2	0.3277	1.5	0.04545	0.87
P301-7	0,01	604	0,62	286.4	±2.6	22.01	0.94	0.05145	1.8	0.3223	2	0.04543	0.94
P301-8	0,04	808	0,65	292.1	±2.6	21.57	0.91	0.05246	1.4	0.3353	1.7	0.04635	0.91

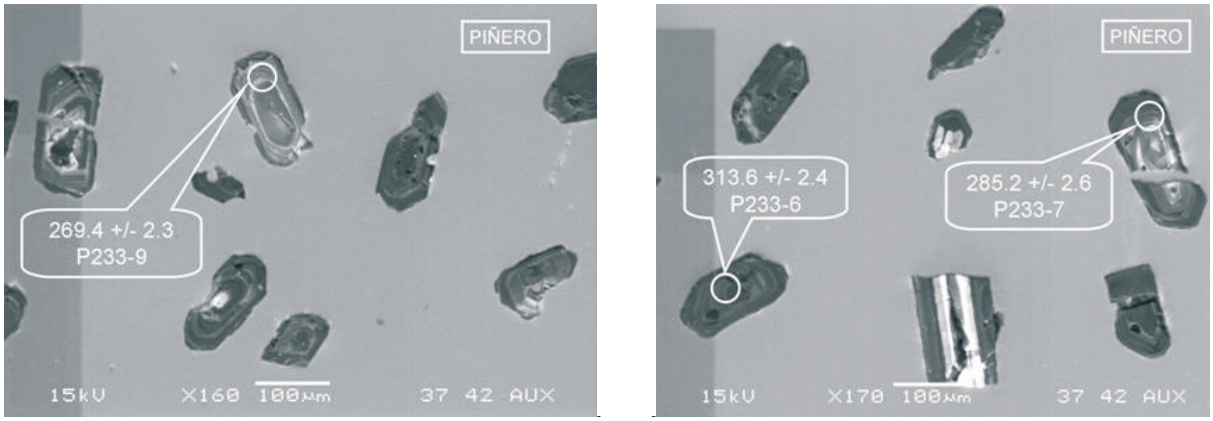

Figure 6. Selected zircon SEM images for Piñero Granite (P233) samples.

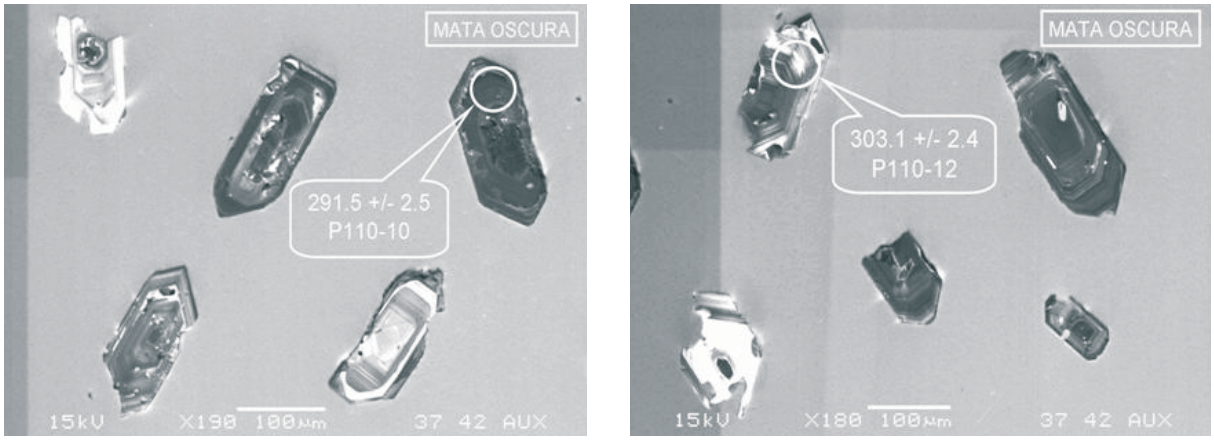

Figure 7. Selected zircon SEM images for Mata Oscura Granite (P110) samples.

Table 3
Piñero Granite (P233) isotopic SHRIMP-RG zircon data

Spot	% $^{206}Pb_c$	ppm U	$^{232}Th/^{238}U$	$^{206}Pb/^{238}U$ Age		$^{238}U/^{206}Pb^*$	±%	$^{207}Pb^*/^{206}Pb^*$	±%	$^{207}Pb^*/^{235}U$	±%	$^{206}Pb^*/^{238}U$	±%
P233-1	0,26	2688	0,66	291.2	±2.3	21.64	0.82	0.05323	0.9	0.3392	1.2	0.04622	0.82
P233-2	0,05	1015	0,79	294.2	±2.5	21.42	0.88	0.05257	1.2	0.3384	1.5	0.04669	0.88
P233-3	2,72	2712	0,78	136.8	±1.2	46.61	0.88	0.052	3.6	0.1538	3.7	0.02145	0.88
P233-4	2,56	4046	0,52	294.2	±3.2	21.42	1.1	0.0585	15	0.377	16	0.04669	1.1
P233-5	0,74	1039	0,86	237.7	±2.1	26.62	0.9	0.0522	2.8	0.2702	2.9	0.03756	0.9
P233-6	0,04	9582	0,91	313.6	±2.4	20.06	0.79	0.05281	0.41	0.3629	0.89	0.04984	0.79
P233-7	-	778	0,73	285.2	±2.6	22.11	0.95	0.05092	1.5	0.3176	1.8	0.04523	0.95
P233-8	4,09	4089	1,24	271.4	±2.3	23.26	0.87	0.0527	6.9	0.312	7	0.04299	0.87
P233-9	0,35	1442	0,59	269.4	±2.3	23.43	0.86	0.05136	1.8	0.3022	2	0.04268	0.86
P233-10	0,20	718	0,89	288.2	±2.6	21.87	0.92	0.05364	1.4	0.3382	1.7	0.04572	0.92
P233-11	0,13	470	0,68	287.5	±2.8	21.93	0.98	0.05309	1.8	0.3338	2	0.0456	0.98
P233-12	0,66	2163	0,45	287.5	±2.4	21.93	0.84	0.051	3.4	0.321	3.5	0.04561	0.84

Table 4
Mata Oscura Granite (P110) isotopic SHRIMP-RG zircon data

Spot	% $^{206}Pb_c$	ppm U	$^{232}Th/^{238}U$	$^{206}Pb/^{238}U$ Age		$^{238}U/^{206}Pb^*$	±%	$^{207}Pb^*/^{206}Pb^*$	±%	$^{207}Pb^*/^{235}U$	±%	$^{206}Pb^*/^{238}U$	±%
P110-1	0,02	1476	0,79	287.3	±2.4	21.95	0.85	0.05138	1.3	0.3228	1.5	0.04557	0.85
P110-2	0,09	1764	1,21	297	±2.4	21.21	0.84	0.05171	1.2	0.3361	1.5	0.04714	0.84
P110-3	1,17	289	1,15	157.5	±2	40.43	1.3	0.0461	9.9	0.157	10	0.02473	1.3
P110-4	0,07	3064	0,68	301.7	±2.4	20.87	0.81	0.05231	0.86	0.3455	1.2	0.04791	0.81
P110-5	0,20	1392	0,50	287	±2.4	21.97	0.86	0.0527	1.3	0.3308	1.5	0.04552	0.86
P110-6	-	2085	1,13	295.4	±2.4	21.33	0.83	0.05185	0.92	0.3352	1.2	0.04689	0.83
P110-7	1,14	2459	0,53	277.6	±2.3	22.73	0.83	0.0534	2.1	0.3238	2.3	0.044	0.83
P110-8	0,35	769	0,78	274.7	±2.5	22.97	0.92	0.052	2.3	0.3119	2.5	0.04354	0.92
P110-9	7,10	562	0,76	293.6	±3.5	21.46	1.2	0.046	13	0.295	14	0.0466	1.2
P110-10	0,12	1259	0,84	291.5	±2.5	21.62	0.86	0.05286	1.3	0.3371	1.6	0.04625	0.86
P110-11	0,12	1862	0,94	291.7	±2.4	21.6	0.84	0.0531	0.89	0.339	1.2	0.04629	0.84
P110-12	0,04	3936	0,95	303.1	±2.4	20.77	0.81	0.05251	0.66	0.3486	1	0.04815	0.81

(Figure 9), in some cases with an irregular core without a clear definition of inherited zircon. The data points for Mogote Granite (Table 5, Figure 10) are concordant, with a $^{206}Pb/^{238}U$ age of 493.8 ± 5.2 Ma, and that is late Cambrian.

Based on the SEM images that show that the majority of the zircon grains have oscillatory zoning and pyramidal faces we interpret these new dates as intrusion ages.

Conclusions

Five different U-Pb ages were obtained in this study which differ and are systematically older than previous K-Ar and Rb-Sr ages. The new dates allowed placing the rocks units in a new time framework of main orogenic events (Figure 11). The Mogote Granite was intruded during the Taconic orogeny whereas the Mata Oscura and Piñero granites, as well as the Corcovado and Segoviera rhyolites, fall at the end of the Appalachian orogeny. North of the Venezuelan Guyana Shield, the basement rocks exposed on exploratory oil wells of the Barinas-Apure and Guárico sedimentary basins have been recognized as metasedimentary and granitic forming a Paleozoic belt [4].

This has been suggested as product of a tectonic compressive episode [4, 19-22]. The belt was formed at the northern edge of Gondwana, product of continental collision with Laurentia, during the Early Paleozoic, continued with mag-

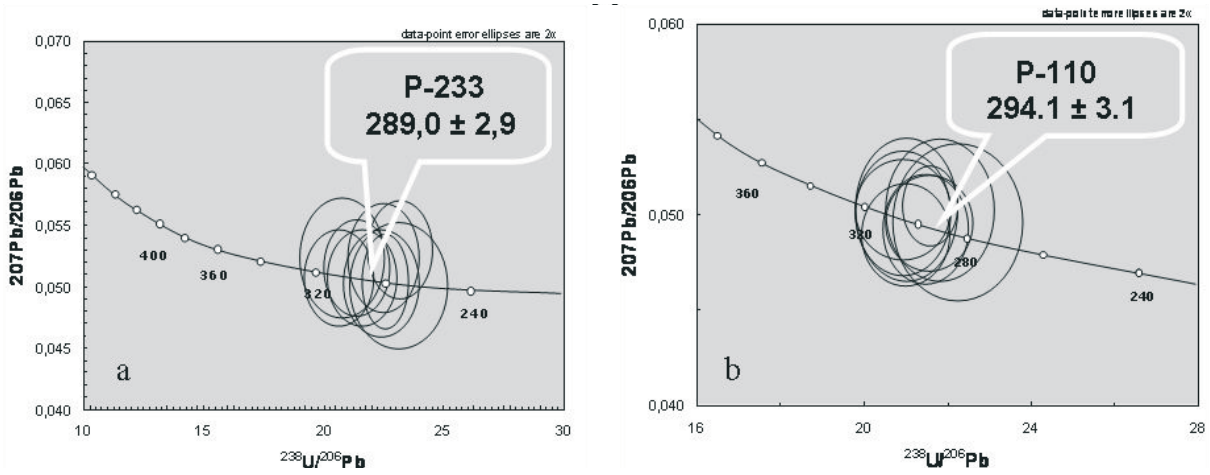

Figure 8. Concordia diagram. (a) Piñero Granite and (b) Mata Oscura Granite.

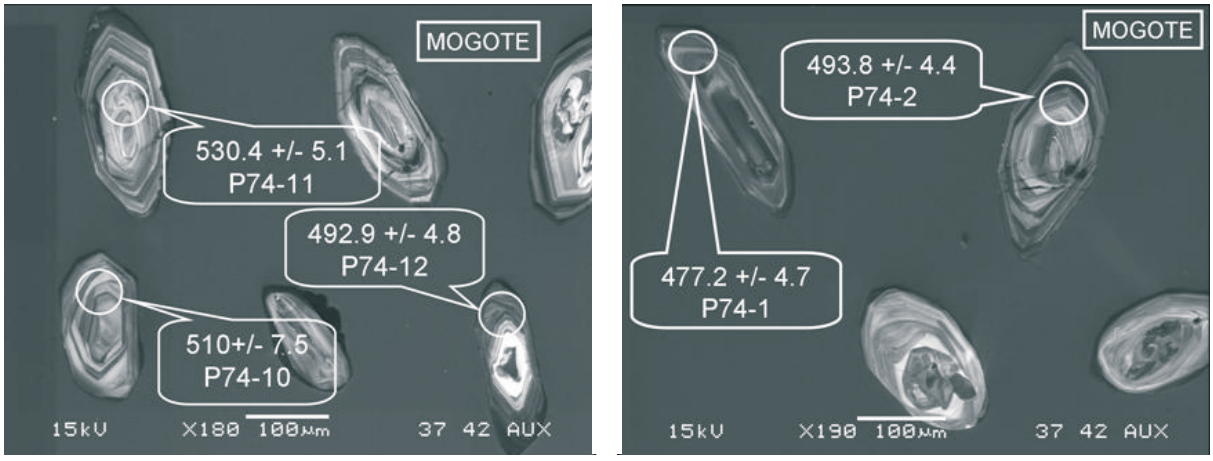

Figure 9. Selected zircon SEM images for Mogote Granite (P74) samples.

Table 5
Mogote Granite (P74) isotopic SHRIMP-RG zircon data

Spot	% $^{206}Pb_c$	ppm U	$^{232}Th/^{238}U$	$^{206}Pb/^{238}U$ Age		$^{238}U/^{206}Pb^*$	±%	$^{207}Pb^*/^{206}Pb^*$	±%	$^{207}Pb^*/^{235}U$	±%	$^{206}Pb^*/^{238}U$	±%
P74-1	0,06	315	0,18	477.2	±4.7	13.01	1	0.0566	1.8	0.6	2.1	0.07684	1
P74-2	0,09	515	0,10	493.8	±4.4	12.56	0.93	0.0578	1.3	0.634	1.6	0.07962	0.93
P74-3	0,04	549	0,10	498.5	±4.4	12.44	0.92	0.05754	1.2	0.6378	1.5	0.0804	0.92
P74-4	-	627	0,10	518.7	±4.5	11.93	0.91	0.05662	1.2	0.6541	1.5	0.08379	0.91
P74-5	0,15	397	0,12	476.6	±4.5	13.03	0.98	0.05723	1.7	0.605	2	0.07673	0.98
P74-6	0,01	391	0,13	489.8	±4.6	12.67	0.97	0.05703	1.5	0.621	1.8	0.07894	0.97
P74-7	0,11	371	0,17	497.1	±4.7	12.47	0.99	0.0576	1.6	0.637	1.9	0.08017	0.99
P74-8	-	555	0,13	512.7	±4.5	12.08	0.92	0.05697	1.2	0.65	1.6	0.08278	0.92
P74-9	0,10	174	0,63	490.6	±5.5	12.65	1.2	0.0578	2.2	0.63	2.5	0.07907	1.2
P74-10	0,04	75	0,93	510	±7.5	12.15	1.5	0.0578	3.3	0.656	3.7	0.0823	1.5
P74-11	0,01	366	0,48	530.4	±5.1	11.66	0.99	0.0565	2.1	0.669	2.3	0.08577	0.99
P74-12	0,19	343	0,14	492.9	±4.8	12.58	1	0.0572	1.9	0.627	2.2	0.07947	1

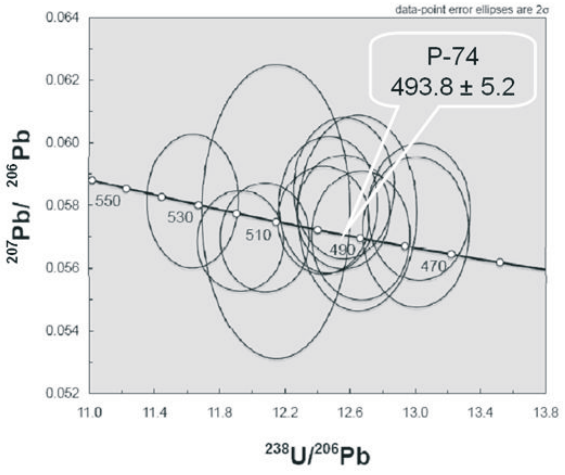

Figure 10. Concordia diagram. Mogote Granite.

matic activity in Late Paleozoic time, related with the Pangea suturing. This folded Palaeozoic belt of Northern South America is also well documented in the Colombian Central Cordillera and well exposed in the Eastern flank of the Santander Massif [23], and includes volcanic and other metamorphic rocks with radiometric determinations ranging from 433 to 277 Ma in age [4].

These new ages lead to an interpretation of the El Baúl massif fully as part of a Paleozoic basement belt. We now rather correlate El Baúl granitoids with the igneous rocks of the Mérida Andes [24, 25], the granodiorite pluton of Paraguaná [26] and the igneous rocks under the sedimentary basins [19]. The geology of El Baúl

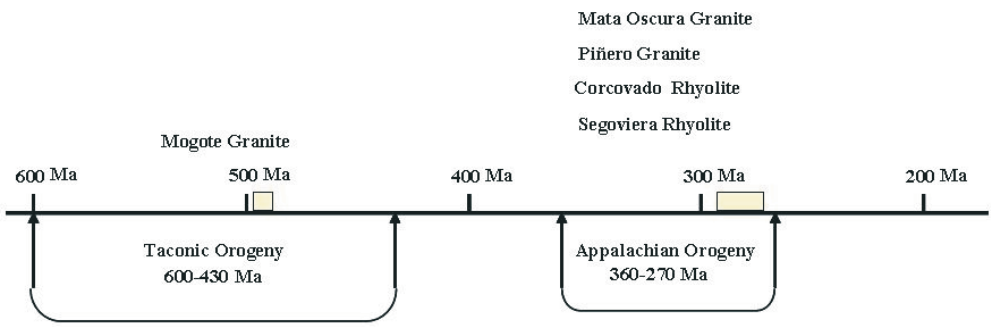

Figure 11. Dated rhyolite and granite units in the main orogenies age framework.

shows more affinity with the Mérida Andes [27] than an "Arch" spreading from the Guyana shield up to peninsula of Paraguaná.

The new results show two magmatic pulses, and hereby, we suggest: 1) The Late Cambrian Mogote Granite age represents an early magmatic-granitic event of the Paleozoic belt. Probably the Mogote Granite intruded (Taconic orogeny) Hato Viejo and Carrizal formations (Early Cambrian), older than El Barbasco sedimentation (Ordovician), which covers a Precambrian basement of Parguazensis age (1545 ± 20 Ma). This Cambrian pericratonic basement was part of the northwestern edge of the Gondwana proto-margin [28], including the Santander Massif. 2) Rocks of Early Permian ages (Piñero and Mata Oscura granites) were emplaced at swallow depth of the cortical block, in a relatively quiescent period at the end of the Appalachian orogeny, together with an Early Permian rhyolitic lava flow event of the Guacamayas volcanics, therefore they both could be part of the same mayor igneous event, emplaced in deep to shallow environments. Rhyolitic dikes from this last event also cut the metasedimentary and granitic units. Fission track dating would be advisable to better understand the exhumation history of the massif.

Acknowledgments

We thank the Council of Scientific, Humanistic and Technological Development of the Andes University (CDCHT-ULA) in Mérida, Venezuela, the GEODINOS (Geodynamics of Northern South America) project (G-2002000478) led by the Venezuelan Foundation of for Seismological Research (FUNVISIS) and the Institute of Earth Sciences (ICT) from the Venezuelan Central University (UCV) in Caracas. We are also grateful to the Laboratory of Isotope Geology at The University of Georgia and the Sensitive High Mass-Resolution Ion Microprobe (SHRIMP-RG) team at Stanford University, California (USA).

References

1. Martín de Bellizzia, C. 1961. Geología del macizo de El Baúl, estado Cojedes. Memoria III Congreso Geológico Venezolano. Noviembre 1959, Bol. de Geol. (Caracas), Publ. Esp. 3(4):1463-1530.
2. Centro de Procesamientos Digital de Imágenes-CPDI. 2004. Imágenes diversas disponibles en htpp://cpdi.fii.org
3. Bellizzia, A., N. Pimentel, and R. Bajo. 1976. Mapa geológico-estructural de Venezuela. Min. Minas e Hidrocarburos, Div. Exploraciones Geológicas y FONINVES. Map scale 1:500.000.
4. Feo-Codecido, G., F. Smith, N. Aboud, and E. Di Giacomo. 1984. Basament and Paleozoic rocks of the Venezuelan Llanos basins. Geol. Soc. of Amer. Memoir 162: 175-187.
5. NACSN-North American Commission on Stratigraphic Nomenclature, 2005. North American Stratigraphic Code. AAPG Bulletin 89(11): 1547-1591.
6. Urbani, F. 2005. Nomenclatura y síntesis de las unidades ígneo-metamórficas de la Cordillera de la Costa. Geos 38: 41 + 23 p. in CD. Caracas: Universidad Central de Venezuela.
7. Feo-Codecido, G. 1963. Notes to accompany the Venezuelan contribution to the addition of a World Geological Map scale 1:5 000 000. Bol. Inf. Asoc. Venezolana Geol., Min., Pet. 6(10): 290-307.
8. Macdonald, W. D., and N. D. Opdike. 1974. Triassic paleomagnetism of Northern South America. AAPG Bulletin 58(2):208-215.
9. Carson, C.J., R.G. Berman, R.A. Stern, B.M. Sanborn, T. Skulski, and H.A.I. Sandeman. 2004. Age constrains on the Paleoproterozoic tectonometamorphic history of the Committee Bay region, western Churchill Province, Canada; evidence from zircon and in situ monazite SHRIMP geochronology. Can. Jour. of Ear. Sci. 41(9):1049-1076.
10. Geyh, M.A., and H. Schleicher. 1990. Absolute age determination. Physical and chemical dating methods and their applications. Springer-Verlag 508p.
11. Williams, I. S. 1998. Chapter 1: U-Th-Pb Geochronology by Ion Microprobe. In: McKibben, M. A., Shanks III, W.C., Ridley, W.I. (Eds.), Applications of Microanalytical Techniques to Understanding Mineralizing Processes. Rev. in Econ. Geol. 7:1-35.

12. Ludwig, K.R. 2003. Isoplot/Ex version 3.00. A geochronological toolkit for Microsoft Excel. Berkeley Geochronology Center Special Publication 4:73.

13. Compston, W., I. S. Williams, and C. Meyer. 1984. U-Pb geochronology of zircons from lunar breccia 73217 using a sensitive high mass-resolution ion microprobe. Jour. of Geoph. Res., Supplement 89:B525–B534.

14. Compston, W., I.S. Williams, J.L. Kirschvink, Z. Zhang, and M.A. Guogan. 1992. Zircon U-Pb ages for the Early Cambrian time-scale. Jour. of the Geo. Soc. of London 149:171-184.

15. Pidgeon, R.T., D. Furfaro, A.K. Kennedy, A.A. Nemchin, W. van Bronswijk, and W.A. Todt. 1994. Calibration of zircon standards for the Curtin SHRIMP II. Abstracts of Eighth International Conference on Geochronology, Cosm. and Isot. Geol. 251.

16. Roddick, J.C. 1987. Generalized numerical error analysis with applications to geochronology and thermodynamics: Geoch. et Cosmo. Act. 51:2129-2135.

17. Stern, R.A. 1997. The GSC Sensitive High Resolution Ion Microprobe (SHRIMP): analytical techniques of zircon U-Th-Pb age determinations and performance evaluation. Age and Isotopic Studies: Report 10, Geol. Sur. of Can., Current Research 1997-F, 1-31.

18. Krogh, T.E. 1982. Improved accuracy of U-Pb zircon ages by the creation of more concordant systems using an air abrasion technique. Geoch. et Cosmo. Act. 46:637-649.

19. Smith, F. 1980. El basamento y las rocas paleozoicas en la parte norte de Venezuela. Caracas. Corpoven S.A. Unpublished company report.

20. Bartok, P. 1993. Pre-breakup geology of the Gulf of Mexico-Caribbean: Its relation to Triassic and Jurassic rift systems of the region: Tect. 12: 441- 459.

21. Audemard F. 1991. Tectonics of western Venezuela. Rice University. Houston, Texas. Thesis submitted for the degre Doctor of Philosophy. Unpublished PhD dissertation.

22. Duerto L., A. Pico & P. Bastos. 2007. Tectonic History of Espino Graben, central Venezuela: A new perspective. PDVSA-Exploración. División Oriente. Puerto La Cruz. Venezuela. Unpublished company report.

23. Irving, E.M. 1975. The structural evolution of the northernmost Andes of Colombia. Bol. Geol., Ingeominas 19: 89.

24. González de Juana, C., M. I. Arozena & C. Picard. 1980. Geología de Venezuela y sus cuencas petrolíferas. Ed. Foninves, Caracas 3:911.

25. Case, J. E., and T. L. Holcombe. 1986. Geologic-tectonic map of the Caribbean region. U.S. Geological Survey, Mapa escala 1:2 500 000.

26. Feo Codecido, G., B.C. Martín, & P. Bartok. 1974. Guía de la excursión a la Península de Paraguaná. Asoc. Venez. de Geol., Min. y Pet. 33.

27. Teggin, D. 1984. Determinaciones radiométricas de edad en los Andes venezolanos. Act. Cien. Venez. 35:374-381.

28. Mendoza, V. 2005. Geología de Venezuela. 2:1: Escudo de Guayana, Andes venezolanos y Cordillera de La Costa. Geos 38:121-122 + 418 p. in CD. Caracas: Universidad Central de Venezuela.

Recibido el 16 de Abril de 2009

En forma revisada el 21 de Septiembre de 2009